Statistical *Ab Initio* Analysis of Electron Trapping Oxide Defects in the Si/SiO_2 Network

Christoph Wilhelmer[1], Markus Jech[1], Dominic Waldhoer[1,2], Al-Moatasem Bellah El-Sayed[1,3], Lukas Cvitkovich[1] and Tibor Grasser[1]
[1]Institute for Microelectronics, Technische Universität Wien,
Gußhausstraße 27–29, 1040 Vienna, Austria
[2]Christian Doppler Laboratory for Single-Defect Spectroscopy in Semiconductor Devices at the Institute for Microelectronics,
[3]Nanolayers Research Computing, Ltd., 1 Granville Court, Granville Road, London N12 0HL, United Kingdom

E-mail: [wilhelmer | jech | waldhoer | el-sayed | cvitkovich | grasser]@iue.tuwien.ac.at

ESSDERC 2021 - IEEE 51st European Solid-State Device Research Conference (ESSDERC) | 978-1-6654-3748-6/21/$31.00 ©2021 IEEE | DOI: 10.1109/ESSDERC53440.2021.9631833

***Abstract*—It is well established that oxide defects are a major threat concerning the reliability of electronic devices. Point defects like the oxygen vacancy and hydrogen related defects like the hydrogen bridge and the hydroxyl-E' center can trap charges from the Si substrate during operation. Here we present a statistical study of parameters by analyzing 144 defects of each type in amorphous SiO_2. We use density functional theory in conjunction with a hybrid functional to provide a large and accurate dataset of defect parameters such as the relaxation energy or the charge transition level and link them to bias temperature instability in nMOSFET devices.**

***Index Terms*—BTI, nMOS, SiO_2, hydroxyl-E'**

I. Introduction

Point defects have received significant interest over the past decades due to their various implications related to reliability issues [1]. For example, oxide defects in metal oxide semiconductor field effect transistor (MOSFET) devices are suspected to be responsible for bias temperature instability (BTI) [2] and random telegraph noise (RTN) [3] by capturing charges from the substrate during operation. The involved charge transition mechanisms causing BTI can be described by a nonradiative multi-phonon (NMP) process [4]. However, experimental and theoretical studies are still challenging due to the amorphous nature of the oxide, as properties of defects vary over a broad range and can thus only be treated in a statistical manner. Although HfO_2 is more and more used as the gate oxide in modern MOSFETs, even in ultra-scaled devices, an interfacial layer of SiO_2 persists to ensure good lattice matching to Si [5] and thus defect studies in the Si/SiO_2 network remain highly relevant as these defects are closest to the channel and therefore dominate the observed charge trapping.

Among the various defect types, the oxygen vacancy (OV) is the most investigated defect candidate in a-SiO_2. Studies have clearly shown, however, that the OVs charge transition levels are far outside a reasonable interaction window regarding the charge exchange with carriers in the Si substrate [6]. Nevertheless, hydrogen atoms, which are deliberately introduced into the device during annealing [7], can easily diffuse through the oxide and interact with already existing OVs to form a new defect type, the so-called hydrogen bridge (HB), with its trap levels near the band edges of Si. Another previously discovered defect candidate is the hydroxyl-E' center (H-E') [8], where a hydrogen atom breaks a strained Si-O bond

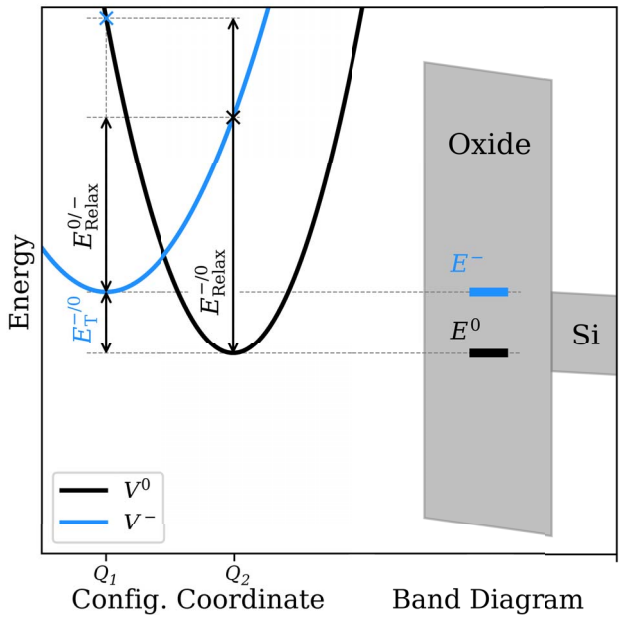

Fig. 1. Schematics of the potential energy surfaces (PES) V^0 and V^- in the harmonic approximation for an oxide defect in two charge states 0 and $-$ as a function of the configuration coordinate (left). The energy levels are shown within the context of the band diagram of a Si/SiO_2 network (right), with the minimum of the negative PES, E^-, assumed as the energy reference fixed at the conduction band edge. The energy difference $E^- - E^0$ is defined as the thermodynamic trap level $E_T^{-/0}$.

in SiO_2, forming a Si dangling bond facing a hydroxyl group. Even though these defects and their effect on pMOS device reliability have been investigated over the last years [9], a consistent theoretical study of their electron trapping properties is still missing. Here we use density functional theory (DFT) employing a hybrid functional to calculate properties for neutral and negatively charged defects on a statistical level. The initial, amorphous SiO_2 structures were created by performing a melt-and-quench procedure using a molecular dynamics algorithm and consecutive DFT cell optimizations. We statistically analyze charge transitions at the defect site by calculating the relaxation energies and charge transition levels of 144 initial defects of each kind introduced above as shown in Fig. 1. We show that the -/0 charge transition

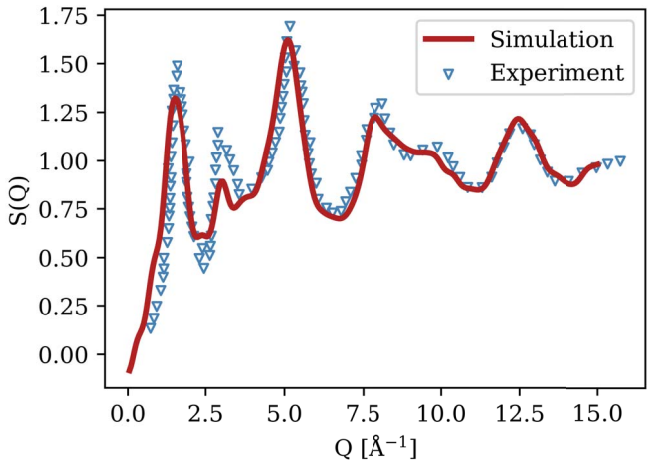

Fig. 2. Structure factor S, as a function of the scattering vector Q for the utilized structure used for defect calculations compared to experimental data [10].

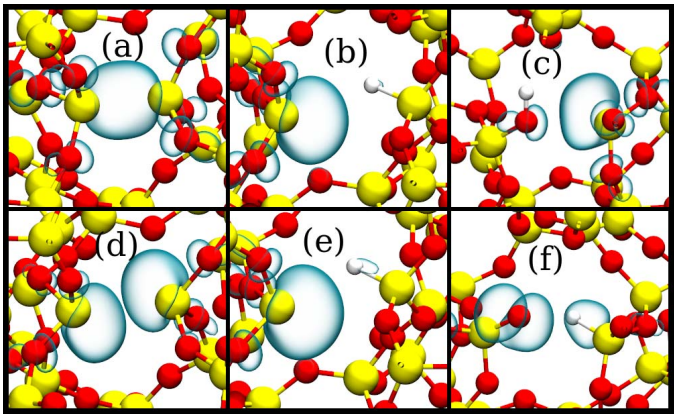

Fig. 3. Examples of the a-SiO_2 defect candidates, oxygen vacancy (left), hydrogen bridge (middle) and hydroxyl-E' center (right), in the neutral (top) and negative (bottom) charge states with their HOMO localized at the defect site.

levels of the hydrogen related defects are normally distributed in the vicinity of the conduction band edge of the Si substrate which renders them compatible to experimental investigations of RTN and PBTI in nMOS devices.

II. Methodology

A. DFT Setup

First-principle calculations were performed with periodic boundary conditions using the Gaussian plane wave (GPW) method as implemented in the CP2K code [11]. A double-ζ Gaussian basis set [12] was employed in combination with the Goedecker-Teter-Hutter (GTH) pseudopotentials [13] and an energy cutoff of $800\,\mathrm{Ry}$. We use the non-local hybrid functional PBE0_TC_LRC [14] for all calculation to minimize the errors of electronic state calculations and set the convergence criteria for the SCF cycle to $2.7\times10^{-6}\,\mathrm{eV}$. In addition, the auxiliary basis set pFIT3 [15] was employed to make calculations of the Hartree-Fock exchange, necessary for hybrid functionals, computationally more feasible. The Broyden-Fletcher-Goldfarb-Shanno (BFGS) algorithm was used to perform geometry optimizations in different charge states.

B. Structure creation

We employ the melt-and-quench procedure [6] to the crystalline SiO_2 polymorph β-cristobalite to create 20 structures of amorphous SiO_2 with 216 atoms each. β-cristobalite was chosen since its density ($2.33\,\mathrm{g\,cm^{-3}}$) is closest to the experimental value of a-SiO_2 thin films ($2.18\,\mathrm{g\,cm^{-3}}$) [16] compared to other polymorphs like α-Quartz ($2.65\,\mathrm{g\,cm^{-3}}$). The structures were created with a molecular dynamics (MD) algorithm as implemented in the LAMMPS code [17] with the classical ReaxFF potential [18]. This force field was successfully used in previous publications [19] [20] due to its ability to describe dynamic bond formation and breakage. For all MD calculations, the time step was set to $0.1\,\mathrm{fs}$ and the thermostat and barostat parameters were chosen to keep the root mean squared fluctuations below 10^{-5}. The β-cristobalite was heated above its arteficial melting point to $5000\,\mathrm{K}$ and equilibrated at this temperature for $1\,\mathrm{ns}$ and cooled down subsequently to $0\,\mathrm{K}$ at a cooling rate of $6\,\mathrm{K\,ps^{-1}}$. Consequently, we performed cell optimizations on the quenched structures within DFT to lower the internal forces to $0.025\,\mathrm{eV/Å}$ and to reduce the pressure to $0\,\mathrm{GPa}$ within a tolerance of $0.01\,\mathrm{GPa}$.

C. Structural Analysis

The structures created using the procedure described above resemble important characteristics of realistic a-SiO_2. The bond lengths ($1.63\pm0.015\,$Å) and angles (O-Si-O = $109.47\pm4.261\,^\circ$ and Si-O-Si = $143.41\pm13.203\,^\circ$) agree well with high-energy X-ray and neutron diffraction data [21] and are in the same range as previous DFT calculations [20]. The mass density is also in very good agreement with experiments ($\rho = 2.17\,\mathrm{g\,cm^{-3}}$) [16].

As Bragg's law cannot be applied in amorphous materials, the structure factor [22] is preferably used in amorphous materials to characterize the short-, medium- and long-range order. The structure factor of our model structure used for defect calculations compares very well to neutron diffraction data [10] over the whole Q range as shown in Fig. 2.

III. Defect Candidates

The three defect candidates studied in this work, oxygen vacancy, hydrogen bridge and hydroxyl-E' center, are shown in Fig. 3 (a-f) together with their corresponding charge distribution for the highest occupied molecular orbital (HOMO) for the neutral and negative charge state. A detailed description of these defects can be found in [23]. For all three defect types, puckered configurations are also discussed, where a silicon atom moves through the plane of its three adjacent O atoms and often back-bonds to a fourth O atom.

OVs were created by removing a single O atom from the structure. For the HBs, an O was replaced by an H atom, while for the H-E' a H atom was placed in the vicinity of an O. 144 initial defect structures of each kind were created in this way

and geometry optimizations were performed on them using the DFT setup described in the previous section.

IV. Relaxation Energies

In the following, the relaxation energy is denoted as $E^{0/-}_{\mathrm{Relax}}$ and $E^{-/0}_{\mathrm{Relax}}$ for the transitions $0 \rightarrow -$ and $- \rightarrow 0$ respectively as shown in Fig. 1. To calculate E_{Relax} of the accumulated defects, single point calculations were performed at charge state $-$ (0) on the relaxed configuration in the opposite charge state 0 ($-$). $E^{0/-}_{\mathrm{Relax}}$, for example, can afterwards simply be calculated as the energy difference to the relaxed configuration in the new charge state:

$$E^{0/-}_{\mathrm{Relax}} = V^{-}(Q_2) - V^{-}(Q_1) \tag{1}$$

with Q_1 and Q_2 being the equilibrium positions of the defect configuration in charge state $-$ and 0, respectively.

The obtained relaxation energies for each defect type are summarized in Fig. 4. The sample size of the E_{Relax} distributions differs because a certain number of the single point calculations did not meet the required convergence criteria. The majority of the relaxation energies of the oxygen vacancies is distributed below 2 eV. Only puckered OVs have relaxation energies > 3 eV. For the HB, E_{Relax} for both charge transitions are asymmetrically distributed between 1 and 3 eV with a peak at around 1.5 eV. E_{Relax} of the H-E' resembles a normal distribution for the 0/$-$ transition with the peak at 2 eV, while for the $-$/0 transition the relaxation energies are between the energy range 1-2 eV for all analyzed defects.

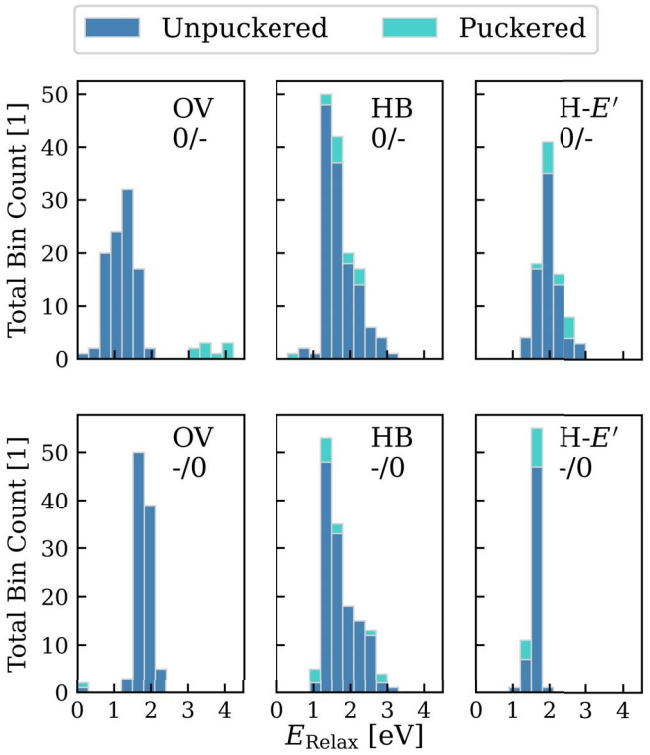

Fig. 4. Calculated relaxation energies for three defect types: Oxygen vacancy, hydrogen bridge and hydroxyl-E' center.

V. Charge Transition Levels

The charge transition level (CTL) can be calculated by comparing the formation energy of a defect in two charge states. The formation energy of a defect in charge state Q is given by

$$E^{\mathrm{Q}}_{\mathrm{Form}}(R) = E^{\mathrm{Q}}_{\mathrm{tot}}(R) - E^{\mathrm{bulk}}_{\mathrm{tot}} - \sum_i \mu_i n_i + Q E_{\mathrm{F}} + E^{\mathrm{cor}} \tag{2}$$

where $E^{\mathrm{Q}}_{\mathrm{tot}}$ is the total energy of the system with the defect in charge state Q, $E^{\mathrm{bulk}}_{\mathrm{tot}}$ is the total energy of the defect-free neutral bulk, $\mu_i n_i$ stands for the chemical energy needed to add or remove atoms of kind i to the bulk to create the defect, E_{F} is the Fermi level and E^{cor} is a correction term necessary for DFT calculations of charged systems within periodic boundary conditions. The Fermi level is calculated with respect to the valence band maximum $E_{\mathrm{F}} = E_{\mathrm{VBM}} + \epsilon_{\mathrm{F}}$. Here, E_{VBM} is approximated as the highest occupied Kohn-Sham orbital of the defect-free bulk structure [24]. The correction term E^{cor} has been calculated to 0.35 eV for our structures within the image charge correction scheme of Makov and Payne [25].

The CTL corresponds to the Fermi level where the charged and the neutral formation energies are equal and thus both charge states are equally stable. It is a key characteristic of a defect, as the trap level with respect to the Fermi level determines the thermodynamically preferred charge state. The position of the trap level can be shifted by applying a gate bias due to the occurring electric field in the oxide and band bending near the interface. As the probability of the defect to capture charges from the substrate can be altered, the CTL is detectable experimentally and thus can be used to identify defects based on measurements. The CTL distributions in the band gap of SiO_2 for electron capture for defect types OV, HB and H-E' are shown in Fig. 5 with the calculated band gap of the Si bulk indicated as a gray area. The CTLs for all defect types resemble normal distributions with parameters given in Fig. 5. The majority of CTLs for the OV are above the Si conduction band edge. Only the puckered configurations possess lower CTLs. Nevertheless, their calculated formation energies are far higher compared to the unpuckered configurations and thus are less likely to occur in a-SiO_2. In comparison to the CTLs of OVs for hole transitions [9] however, the CTLs for trapping electrons are closer to the energy of the relevant charge reservoir and the OV has to be considered as a defect candidate for trapping electrons from the substrate. For the HB and H-E', the CTLs are distributed around the conduction band edge of the Si substrate and thus these defects are plausible candidates for electron capture processes during operation [1].

VI. Conclusion

We provided a large and consistent data set of relaxation energies and charge transition levels for the $-$/0 charge transition for the three defect candidates in amorphous SiO_2, oxygen vacancy (OV), hydrogen bridge (HB) and hydroxyl-

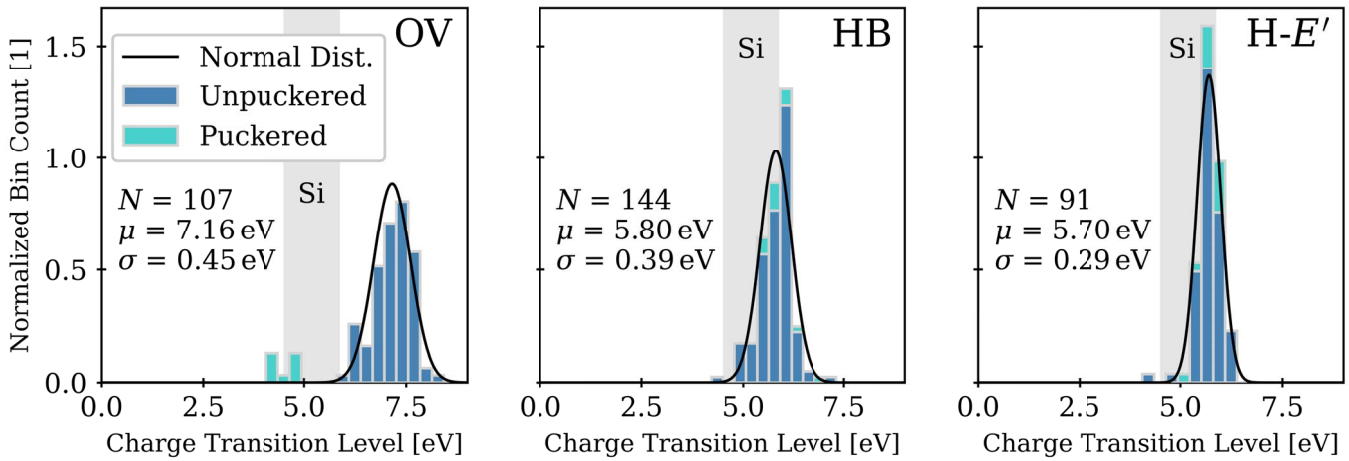

Fig. 5. Charge transition levels of defect types oxygen vacancy (left), hydrogen bridge (HB) and hydroxyl-E' center (H-E') in a-SiO_2 for transition 0/-. A normal distribution was fitted to the data with the fitting parameters given in the plot. The Band gap of Si in a Si/SiO_2 network is indicated by a gray area.

E' center (H-E'), that can be directly linked to experimental characterizations in MOSFET devices. Our calculations show that the charge transition levels (CTLs) of OVs are distributed above the conduction band edge of the Si substrate. Contrary to the +/0 CTLs, some OVs possess trap levels within a reasonable range to interact with the carrier reservoir at high electric field conditions, potentially provoking the effect of bias temperature instability. On the other hand, CTLs of HBs and H-E's are distributed much closer to the Si conduction band edge of Si and hence are possible candidates to explain random telegraph noise under positive bias conditions.

Acknowledgment

This project was funded by the European Union's Horizon 2020 research and innovation program under grant agreement No. 871813, within the framework of the project Modeling Unconventional Nanoscaled DeviceFABrication (MUNDFAB) and the CDL for Single-Defect Spectroscopy in Semiconductor Devices (SDS).

References

[1] G. Rzepa *et al.*, "Comphy — A compact-physics framework for unified modeling of BTI," *Microelectron. Reliab.*, vol. 85, pp. 49–65, 06 2018.
[2] T. Grasser *et al.*, "The paradigm shift in understanding the bias temperature instability: From reaction–diffusion to switching oxide traps," *IEEE Trans. Electron Devices*, vol. 58, no. 11, pp. 3652–3666, 2011.
[3] K. S. Ralls *et al.*, "Discrete resistance switching in submicrometer silicon inversion layers: Individual interface traps and low-frequency ($\frac{1}{f}$) noise,"
[4] F. Schanovsky *et al.*, "A multi scale modeling approach to non-radiative multi phonon transitions at oxide defects in MOS structures," *J. Comput. Electron.*, vol. 11, 09 2012.
[5] T. L. Duan *et al.*, "Characterization of the electronic structure and thermal stability of HfO_2/SiO2/Si gate dielectric stack," *Surf Interface Anal*, vol. 49, no. 8, pp. 776–780, 2017.
[6] Y. Wimmer *et al.*, "Role of hydrogen in volatile behavior of defects in SiO_2-based electronic devices," *Proc. R. Soc. A*, vol. 472, no. 2190, p. 20160009, 2016.
[7] C. Kaneta *et al.*, "Defect states due to silicon dangling bonds at the Si(100)/SiO_2 interface and the passivation by hydrogen atoms," *MRS Proceedings*, vol. 592, p. 39, 1999.
[8] L. Skuja *et al.*, "An increased F_2-laser damage in 'wet' silica glass due to atomic hydrogen: A new hydrogen-related E'-center," *J. Non-Cryst. Solids*, vol. 352, no. 23, pp. 2297–2302, 2006.
[9] W. Goes *et al.*, "Identification of oxide defects in semiconductor devices: A systematic approach linking DFT to rate equations and experimental evidence," *Microelectron. Reliab.*, vol. 87, pp. 286–320, 2018.
[10] D. Price and J. Carpenter, "Scattering function of vitreous silica," *J. Non-Cryst. Solids*, vol. 92, no. 1, pp. 153–174, 1987.
[11] T. D. Kühne et al., "CP2K: An electronic structure and molecular dynamics software package - Quickstep: Efficient and accurate electronic structure calculations," *J. Chem. Phys.*, vol. 152, no. 19, p. 194103, 2020.
[12] J. VandeVondele and J. Hutter, "Gaussian basis sets for accurate calculations on molecular systems in gas and condensed phases," *J. Chem. Phys.*, vol. 127, no. 11, p. 114105, 2007.
[13] S. Goedecker, M. Teter, and J. Hutter, "Separable dual-space Gaussian pseudopotentials," *Phys. Rev. B*, vol. 54, pp. 1703–1710, Jul 1996.
[14] M. Guidon, J. Hutter, and J. VandeVondele, "Robust periodic Hartree-Fock exchange for large-scale simulations using gaussian basis sets," *J. Chem. Theory Comput*, vol. 5, no. 11, pp. 3010–3021, 2009.
[15] M. Guidon *et al.*, "Auxiliary density matrix methods for Hartree-Fock exchange calculations," *J. Chem. Theory Comput.*, vol. 6, 07 2010.
[16] M. Hüppauff *et al.*, "Density, thickness and interface roughness of SiO_2, TiO_2 and Ta_2O_5 films on BK-7 glasses analyzed by x-ray reflection," *Thin Solid Films*, vol. 230, no. 2, pp. 191–198, 1993.
[17] S. Plimpton, "Fast parallel algorithms for short-range molecular dynamics," *J. Comput. Phys*, vol. 117, no. 1, pp. 1–19, 1995.
[18] A. Van Duin *et al.*, "ReaxFF SiO reactive force field for silicon and silicon oxide systems," *J. Phys. Chem. A*, vol. 107, pp. 3803–3811, May 2003.
[19] M. Jech *et al.*, "*Ab Initio* Treatment of Silicon-Hydrogen Bond Rupture at Si/SiO_2 Interfaces," *Physical Review B*, vol. 100, p. 195302, 2019.
[20] A.-M. El-Sayed *et al.*, "Nature of intrinsic and extrinsic electron trapping in SiO_2," *Phys. Rev. B*, vol. 89, p. 125201, Mar 2014.
[21] R. A. B. Devine and J. Arndt, "Si—O bond-length modification in pressure-densified amorphous SiO_2," *Phys. Rev. B*, vol. 35, pp. 9376–9379, Jun 1987.
[22] S. R. Elliott, *Physics of amorphous materials*. New York: Longman Scientific & Technical, 1984.
[23] A.-M. El-Sayed *et al.*, "Theoretical models of hydrogen-induced defects in amorphous silicon dioxide," *Phys. Rev. B*, vol. 92, p. 014107, Jul 2015.
[24] C. G. Van de Walle and J. Neugebauer, "First-principles calculations for defects and impurities: Applications to III-nitrides," *J. Appl. Phys.*, vol. 95, no. 8, pp. 3851–3879, 2004.
[25] G. Makov and M. C. Payne, "Periodic boundary conditions in *ab initio* calculations," *Phys. Rev. B*, vol. 51, pp. 4014–4022, Feb 1995.